AIP Applied Physics Letters

Highly efficient poly(3,4-ethylenedioxythiophene):poly(styrenesulfonate)/Si hybrid solar cells with imprinted nanopyramid structures

Jheng-Yuan Chen, Ming-Hung Yu, Shun-Fa Chang, and Kien Wen Sun

Citation: Applied Physics Letters **103**, 133901 (2013); doi: 10.1063/1.4822116
View online: http://dx.doi.org/10.1063/1.4822116
View Table of Contents: http://scitation.aip.org/content/aip/journal/apl/103/13?ver=pdfcov
Published by the AIP Publishing

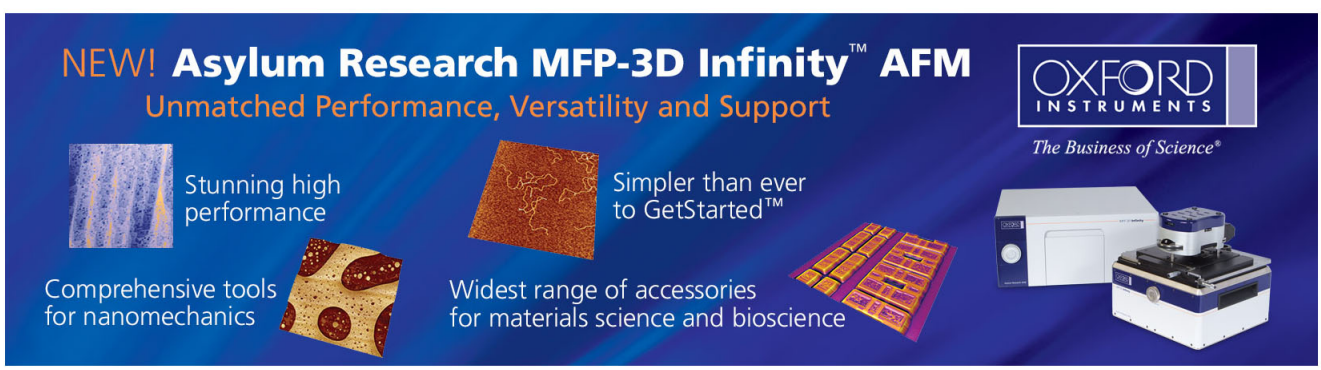

Highly efficient poly(3,4-ethylenedioxythiophene):poly(styrenesulfonate)/Si hybrid solar cells with imprinted nanopyramid structures

Jheng-Yuan Chen, Ming-Hung Yu, Shun-Fa Chang, and Kien Wen Sun[a)]
Department of Applied Chemistry, National Chiao Tung University, 1001 University Road, Hsinchu 30010, Taiwan

(Received 25 July 2013; accepted 8 September 2013; published online 24 September 2013)

High-efficiency hybrid solar cells based on nanostructured silicon and poly(3,4-ethylenedioxythiophene): poly(styrenesulfonate), which were fabricated via a simple nanoimprint fabrication process, demonstrated an excellent power conversion efficiency of 10.86%. The complex and costly high-temperature photolithography and masking steps were replaced by techniques that are low-cost and capable of mass production. The nanopyramid structures fabricated on the silicon surface provided an antireflective effect and have a radial junction architecture that enhanced the light absorption and carrier collection efficiency. The short-circuit current density (J_{sc}) of the hybrid solar cell with nanopyramid structures was greatly improved from 24.5 mA/cm^2 to 32.5 mA/cm^2 compared with that of a flat surface device. The highest solar cell efficiency was achieved on a 525 μm-thick 2.3 Ω cm n-type Czochralski process (CZ) Si substrate with a designated area of 4 cm^2. © *2013 AIP Publishing LLC*. [http://dx.doi.org/10.1063/1.4822116]

Crystalline Si has dominated the photovoltaic markets for years because of its abundant material supply, nontoxicity, and high efficiency. However, the expensive fabrication processes and materials for crystalline Si solar cells limit the wide application of photovoltaics. The fabrication of p-n junctions for Si involves furnace diffusion, which is expensive and requires very high temperatures (~1000 °C). Therefore, hybrid solar cells that combine Si and conjugated polymers at low temperatures provide an alternative to simplify the fabrication processes and reduce costs.[1–9] The conjugated polymer called poly(3,4-ethylenedioxythiophene):poly(styrenesulfonate) (PEDOT:PSS) is the most widely used organic material for hybrid solar cell devices. PEDOT:PSS is transparent, conductive (1000 S/cm), and can produce a Schottky junction with Si.[4–9] Illuminative light is absorbed in the n-type Si, and a hole transport layer in PEDOT:PSS can extract holes generated in the Si substrate out of the device. Thus, the efficiency of the hybrid PEDOT:PSS/Si solar cell is comparable with a conventional Si p-n junction solar cell, in principle. Techniques for improving hybrid PEDOT:PSS/Si solar cell performance have been widely studied and reported, including surface sturctures,[4–6] surface passivation,[6] and the use of additives.[7–9]

The performance of a solar cell is critically dependent on the absorption of incident photons and their conversion to current. More than 30% of the incident light is reflected from the silicon surface back to the air. The surface nanostructures, which are used for antireflective purposes, are useful for gradient refractive index fabrication and design for efficient antireflective structures.[10–16] Nanostructures with surface relief gratings may be understood in terms of a thin film, in which the refractive index changes gradually and continuously from the top of the structure to the bulk materials. Nanoscale surface structures, such as nanowire,[3,6] nanorod,[13] and nanocone,[4] provide enhanced absorption properties via antireflective and light scattering effects and offers a large junction area for charge separation and radial junction architecture. Recently, solar cells with radial junction arrays have been demonstrated to have enhanced charge transport and high light-harvesting capabilities because of the decoupling of light absorption and charge-carrier collection directions.[4,13,14]

Nanostructures can be fabricated using various techniques that involve lithography and etching. Among these techniques, nanoimprint lithography (NIL) has recently emerged as a promising candidate for fabricating nanostructures.[15–18] NIL is a high throughput, high-resolution parallel patterning method, in which a surface pattern of a stamp is replicated into a material via mechanical contact and three-dimensional material displacement. NIL requires only a simple equipment setup. Thus, the processes involved in NIL are low-cost. The local thickness contrast of the molded thin film can be used to pattern an underlying substrate via standard pattern transfer methods and can also be directly applied in places where a bulk modified functional layer is needed. In this study, we demonstrated a hybrid solar cell that comprises a nanostructured n-type Si surface and a PEDOT:PSS layer. The surface structure of Si was engineered by combining NIL and etching processes to form radial junctions and antireflective architectures for enhanced light absorption.

The surface of an n-type Si ⟨100⟩-oriented wafer (with resistivity of 2.3 Ω cm) was first cleaned, followed by deposition of a 100 nm-thick silicon nitride layer as an etching mask via plasma-enhanced chemical vapor deposition (Oxford Instrument, Plasmalab 80 Plus). In this study, NIL was used to pattern a commonly used photoresist SU-8 (MicroChemicals) on the Si substrates. To produce nanoimprints via the UV-curing process, the patterns on the Si master mold were first duplicated on a transparent and flexible polydimethylsiloxane (PDMS, Sylgard 184) mold via a cast-molding method. The patterns on the replicated PDMS mold

[a)]Author to whom correspondence should be addressed. Electronic mail: kwsun@mail.nctu.edu.tw

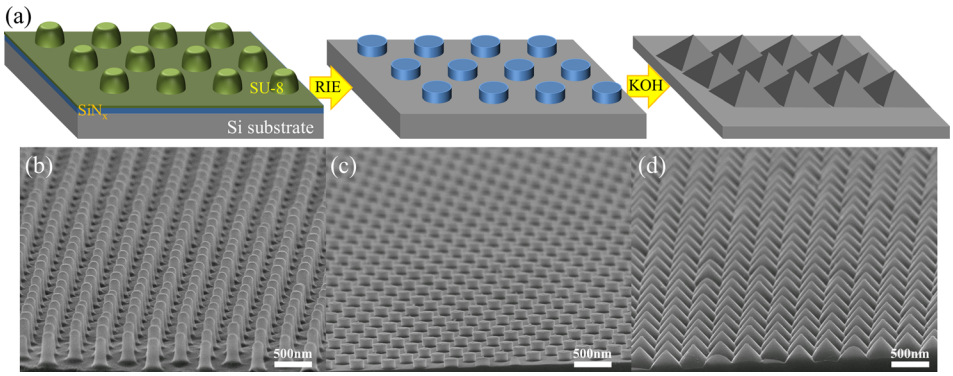

FIG. 1. (a) Schematic of the fabrication process of Si nanopyramid structures. (b) SEM images of the imprinted structures (c) after transferring the patterns into the silicon nitride layer by RIE etching and (d) nanopyramid structures on Si substrate after KOH solution etching.

were then transferred to a substrate coated with SU-8 by using a home-made nanoimprinter at 70 °C and 1 atm for 1 min. After the SU-8 resist completely filled the PDMS mold, the sample was cured using a Xe lamp for 90 s. Figure 1(a) shows the flow chart of the experiments. The SEM image of the imprinted nanostructures on the SU-8 resist with a period of 400 nm and a height of 450 nm is shown in Figure 1(b). The imprinted structures were used as an etching mask to remove the imprinted residual photoresist layer and to transfer the patterns onto the silicon nitride layer by using an inductively coupled plasma-reactive ion etching system. The resulting SEM image of the Si surface is shown in Figure 1(c), where the resist layer was completely removed. Finally, the entire sample was immersed in a potassium hydroxide (KOH) solution mixture composed of 25% KOH and 12.5% isopropyl alcohol (IPA) for 30 s at 80 °C. The wet etching process resulted in tapered nanopyramid arrays on the Si substrate because of the anisotropic etching of the KOH solution.

Figure 2(a) shows the top view SEM image of the nanopyramid structures with the cross-section image displayed in the inset. The Si surface is uniformly covered on a large area with nanostructures that form two-dimensional hexagonal arrays. These arrays have smooth and tapered profiles with a period of 400 nm and a height of 250 nm, which match the Si master mold. The reflectance spectra of the samples with and without the nanopyramid structures were measured and compared using an UV/Visible/NIR spectrophotometer (Hitachi U-4100). The reflection properties of the nanostructure surface were also studied using a rigorous coupled-wave analysis (RCWA). The RCWA approach was employed to analyze the optical diffraction and transmission properties of the nanoscale structures and to solve the Maxwell's equations in a periodic medium after applying the field and permittivity.[10] In this work, a commercial implementation of the three-dimensional RCWA (DiffractMod, Rsoft Corp.) was used. The RCWA simulation was used not only to compare the experiment results but also to optimize the surface nanostructures to achieve an ideal antireflective effect. The simulated reflectance spectra are in agreement with the experimental data, as shown in Figure 2(b). Both calculated and experimental results proved that the nanopyramid structures significantly reduced the surface reflection compared with the flat surface, especially in the short wavelength region.

The processes for fabricating hybrid solar cell devices are as follows: after initial cleaning, the Si substrates with and without the nanopyramid structures were immersed in dilute hydrofluoric (HF) acid (2%) to remove native SiO_2. Immediately after the HF cleaning and drying steps, a 100 nm-thick aluminum layer was deposited on the backside for cathode contact by using an electron beam evaporator. A highly conductive polymer solution was spin-coated on the Si surface by mixing PEDOT:PSS (PH1000 from Clevios) solution with 5 wt. % dimethyl sulfoxide as a secondary dopant to increase the conductivity, followed by thermal annealing at 120 °C for 10 min. The best performance of the hybrid solar cells were achieved at a spin-coating rate of 3000 rpm for the flat surface and 6000 rpm for the nanopyramid structured surface. Finally, a front anode contact was fabricated with a 60-nm-thick silver grid via thermal evaporation through a steel foil shadow mask. The quality of the coated polymer morphology was largely dependent on the spin-coating rates.[5] Figure 3(a) shows the SEM image of the PEDOT:PSS morphology coated on the surface with the nanopyramid structures at a spin-coating rate of 6000 rpm. Even at a spin-coating speed as high as 6000 rpm, small voids are still present at the polymer and Si interface, as shown at the bottom of Figure 3(a). The current density-

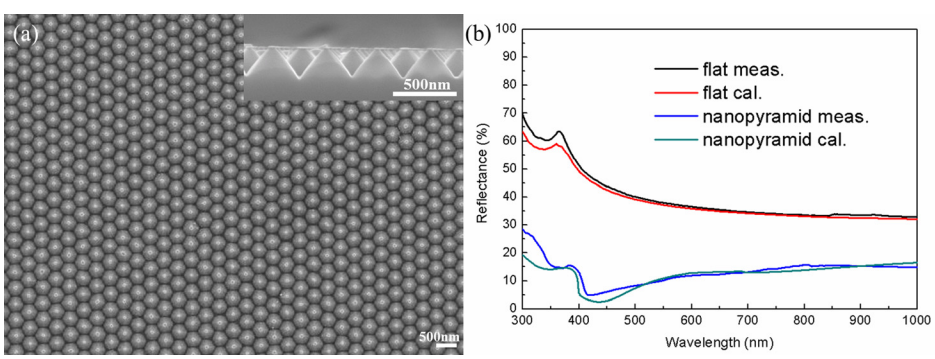

FIG. 2. (a) Top-view and cross-section SEM images of nanopyramid structures. (b) The measured (black and blue curves) and calculated (red and green curves) reflectance spectra with and without the nanopyramid structures.

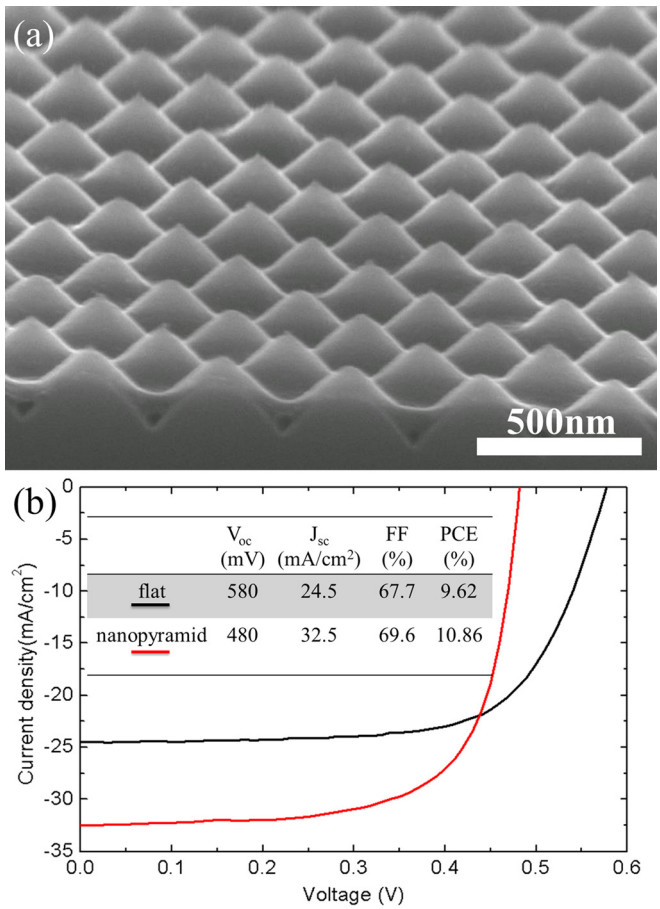

FIG. 3. (a) SEM image of the nanopyramid structures coated with the PEOT:PSS layer. (b) J-V characteristics of the devices with and without the nanopyramid structures.

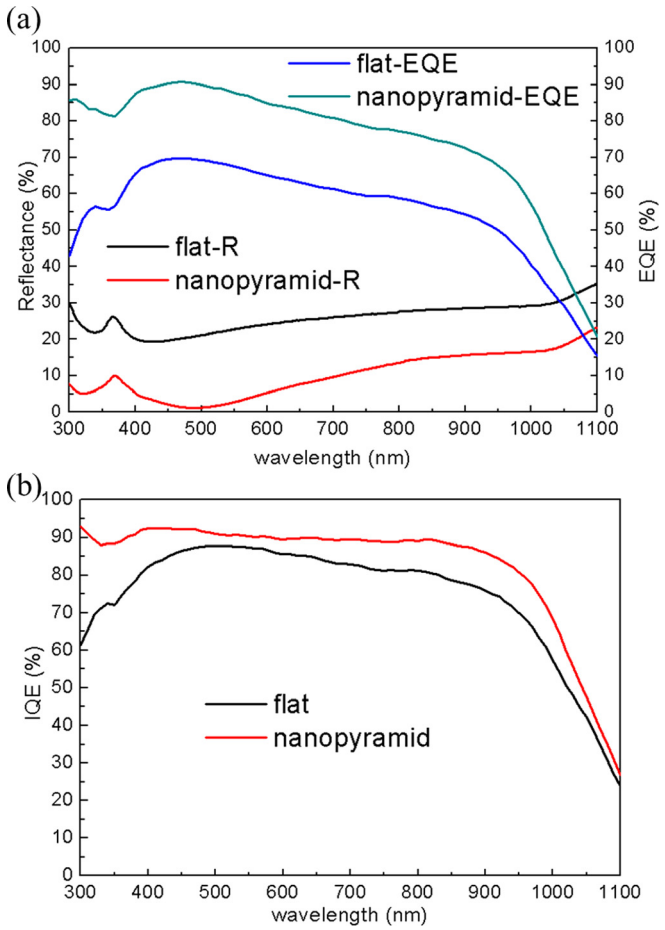

FIG. 4. (a) EQE and reflectance spectra of the hybrid solar cells fabricated at a spin-coating rate of 6000 rpm on the nanopyramid structure surface. A device built on a flat surface at a spin-coating rate of 3000 rpm is displayed in parallel for comparison. (b) The calculated IQE spectra for devices with the flat and nanostructured surface.

voltage characteristics of the devices with and without nanopyramid structures are displayed in Figure 3(b). The device with flat surface was optimized with an open-circuit voltage (V_{oc}) of 580 mV and a power conversion efficiency (PCE) of 9.62% to determine precisely the effects from the nanostructured surface. The structured devices should outperform the efficient flat cell, especially when additional or potential manufacturing costs involved in the structure fabrication process are taken into account. Although V_{oc} dropped to a lower value of 480 mV, the device with nanopyramid structures showed a remarkably enhanced short-circuit current density (J_{sc}) of 32.5 mA/cm^2 and resulted in a high PCE of 10.86%. The decrease in V_{oc} is attributed to the increased interface area and voids [as shown in Figure 3(a)] at the polymer and Si interface, which results in increased surface recombination.[4,5] However, V_{oc} can be further increased at higher spin-coating rates and/or the use of surface passivation with surfactants.

Figure 4(a) shows the measured external quantum efficiency (EQE) and reflectance spectra of the hybrid solar cells fabricated at a spin-coating rate of 6000 rpm on the nanopyramid structures. A device built on a flat surface at a spin-coating rate of 3000 rpm is also displayed in parallel for comparison. A thin PEDOT:PSS layer with a medium refractive index of ~1.48 can reduce the surface reflection when coated on a plain Si. Therefore, combined with the surface nanopyramid structures, the surface reflection of the device is further reduced throughout the entire spectrum. According to the thickness of the PEDOT:PSS layer and its refractive index, the wavelength of the lowest surface reflection shifted from ~420 nm for the surface with nanopyramid structures only [Figure 2(b)] to ~480 nm [Figure 4(a)]. The EQE of the flat surface device reached a maximum of 70% at 470 nm and rapidly decayed toward longer and shorter wavelengths. The solar cell device with nanopyramids clearly outperformed the flat device in EQE throughout the entire wavelength range. The EQE of the nanopyramid device is more than 70% over a wide range (from 300 nm to 1000 nm) and reaches a maximum value of 91% at ~470 nm, which matches the wavelength where the lowest reflection occurs. The internal quantum efficiency (IQE) was also calculated using IQE = EQE/(1 − R) for devices with a back reflector, which describes the wavelength dependence of the charge collection efficiency. The calculated IQE spectra [Figure 4(b)] showed enhancement from surface nanostructures but exclude any anti-reflective effect associated with the surface nanostructures. The discrepancy between this work and the previously reported literature[19] in the short wavelength range (300 nm–400 nm) of the IQE is probably due to the difference in the reflectance. The results from the IQE spectra indicated that the improvement in the EQE and J_{sc} is attributed to the antireflective effect and higher carrier collection

efficiency. The efficient charge transport is due to the radial junction architecture provided by the nanopyramid structures.[14] This result can be explained by the scattering effect of the surface nanopyramid structures, which increases the optical path length inside the Si substrate and enables the light to propagate laterally more easily, thereby allowing absorption to occur close to the surface compared with the flat surface device. The photo-generated carriers are allowed to diffuse to the junction with minimal recombination because of the light trapping effect. Thus, the device shows enhanced response in the whole spectrum range. The surface nanostructures caused strong light absorption and allowed efficient charge transport; thus, the device only requires a thin Si substrate that can further reduce the cost of the solar cells.

In conclusion, we demonstrated the implementation of a PEDOT:PSS/Si hybrid solar cell with imprinted surface nanostructures. The nanopyramid structures on the Si surface, which were fabricated by NIL and KOH etching processes, provide both the anti-reflective effect and radial junction architecture to increase the light absorption and carrier collection efficiency of the solar cells. The NIL technique, together with the KOH solution etching process, provides an economic and simple way of fabricating uniform nanopatterns covering a large area on the Si surface. The J_{sc} and PCE of the hybrid solar cells integrated with nanopyramid structures were enhanced from 24.5 mA/cm^2 to 32.5 mA/cm^2 and from 9.62% to 10.86%, respectively, compared with the flat device. In the future, the V_{oc} of the device can be further improved by reducing the voids at the interface and/or by surface passivation using surfactants.

We would like to thank Professor C. P. Lee at the Department of Electronics Engineering, National Chiao Tung University for the support on the theoretical simulation software. This work was supported by the National Science Council of the Republic of China (Contract No. NSC 101-2918-I-009-002) and the Approaching Top University Program of the Ministry of Education of the Republic of China.

[1]S. Avasthi, S. Lee, Y.-L. Loo, and J. C. Sturm, Adv. Mater. **23**, 5762 (2011).
[2]F. Zhang, B. Sun, T. Song, X. Zhu, and S. Lee, Chem. Mater. **23**, 2084 (2011).
[3]X. Shen, B. Sun, D. Liu, and S.-T. Lee, J. Am. Chem. Soc. **133**, 19408 (2011).
[4]S. Jeong, E. C. Garnett, S. Wang, Z. Yu, S. Fan, M. L. Brongersma, M. D. McGehee, and Y. Cui, Nano Lett. **12**, 2971 (2012).
[5]T.-G. Chen, B.-Y. Huang, E.-C. Chen, P. Yu, and H.-F. Meng, Appl. Phys. Lett. **101**, 033301 (2012).
[6]F. Zhang, D. Liu, Y. Zhang, H. Wei, T. Song, and B. Sun, ACS Appl. Mater. Interfaces **5**, 4678 (2013).
[7]Q. Liu, M. Ono, Z. Tang, R. Ishikawa, K. Ueno, and H. Shirai, Appl. Phys. Lett. **100**, 183901 (2012).
[8]Y. Zhu, T. Song, F. Zhang, S.-T. Lee, and B. Sun, Appl. Phys. Lett. **102**, 113504 (2013).
[9]M. Ono, Z. Tang, R. Ishikawa, T. Gotou1, K. Ueno, and H. Shirai, Appl. Phys. Express **5**, 032301 (2012).
[10]S. Chattopadhyay, Y. F. Huang, Y. J. Jen, A. Ganguly, K. H. Chen, and L. C. Chen, Mater. Sci. Eng. R. **69**, 1 (2010).
[11]Y. Li, J. Zhang, and B. Yang, Nano Today **5**, 117 (2010).
[12]Y. F. Huang, S. Chattopadhyay, Y. J. Jen, C. Y. Peng, T. A. Liu, Y. K. Hsu, C. L. Pan, H. C. Lo, C. H. Hsu, Y. H. Chang, C. S. Lee, K. H. Chen, and L. C. Chen, Nat Nanotechnol **2**, 770 (2007).
[13]Y. Lu and A. Lal, Nano Lett. **10**, 4651 (2010).
[14]J.-Y. Chen, C. Con, M.-H. Yu, B. Cui, and K. W. Sun, ACS Appl. Mater. Interfaces **5**, 7552 (2013).
[15]Q. Chen, G. Hubbard, P. A. Shields, C. Liu, D. W. E. Allsopp, W. N. Wang, and S. Abbott, Appl. Phys. Lett. **94**, 263118 (2009).
[16]J. Y. Chen, W.-L. Chang, C. K. Huang, and K. W. Sun, Opt. Express **19**, 14411 (2011).
[17]L. J. Guo, Adv. Mater. **19**, 495 (2007).
[18]H. Schift, J. Vac. Sci. Technol. B **26**, 458 (2008).
[19]J. Zhang, Y. Zhang, F. Zhang, and B. Sun, Appl. Phys. Lett. **102**, 013501 (2013).